Inorganic Chemistry

Article

pubs.acs.org/IC

Synthesis of Two Triarylboron-Functionalized Metal–Organic Frameworks: In Situ Decarboxylic Reaction, Structure, Photoluminescence, and Gas Adsorption Properties

Xiaoqing Wang,[†] Jie Yang,[†] Liangliang Zhang,[‡] Fuling Liu,[†] Fangna Dai,*[,‡] and Daofeng Sun*[,†,‡]

[†]School of Chemistry and Chemical Engineering, Shandong University, Jinan, Shandong 250100, People's Republic of China

[‡]State Key Laboratory of Heavy Oil Processing, China University of Petroleum (East China), College of Science, China University of Petroleum (East China), Qingdao, Shandong 266580, People's Republic of China

Supporting Information

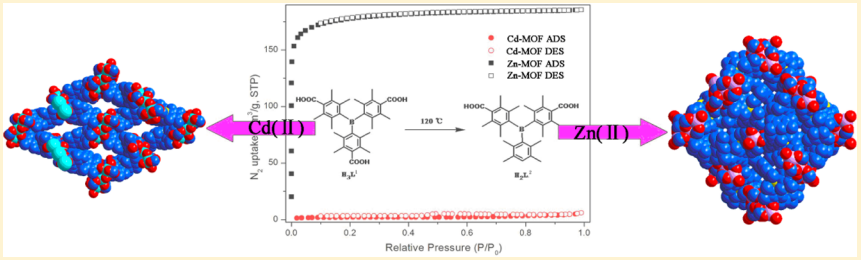

ABSTRACT: Two 3D noninterpenetrating porous metal–organic frameworks (PMOFs) $[Cd_3(\mathbf{L}^1)_2(DMA)_2]\cdot DMA$ [**1**, $H_3\mathbf{L}^1$ = tris(p-carboxylic acid)tridurylborane] and $[Zn_3(\mathbf{L}^2)_3(H_2O)_2]\cdot 5H_2O\cdot 2EtOH$ [**2**, $H_2\mathbf{L}^2$ = 4,4′-((2,3,5,6-tetramethylphenyl)-boranediyl)bis(2,3,5,6-tetramethylbenzoic acid)] were synthesized by employment of a C_3-symmetric ligand ($H_3\mathbf{L}^1$) to assembly with $Cd(NO_3)_2$ or $Zn(NO_3)_2$. Complex **1** exhibits a (3, 6)-connected topological network based on a Cd_3 cluster and Y-shaped trinodal organic linker. Complex **2** shows a 6-connected topology, since in situ decarboxylic reaction of the initial $H_3\mathbf{L}^1$ occurred to generate a new ligand, $H_2\mathbf{L}^2$, which can be considered as a linear linker. Both **1** and **2** exhibit blue fluorescence. Significantly, complex **1** with larger channels is unstable upon the removal of guest molecules. In contrast, activated **2** exhibits higher stability and permanent porosity.

INTRODUCTION

Porous coordination polymers (PCPs) or porous metal–organic frameworks (PMOFs) have attracted enormous attention as an emerging class of microporous materials, which are of fascinating structures and important applications in gas storage and separation, chemical absorption, luminescence, electronics, drug delivery, and catalysis.[1−6] The utilities of PMOFs are mostly attributed to their large internal surface areas and permanent porosities. It is well-known that the construction of PMOFs can be affected by a number of factors, such as building units, temperature, pH, reaction time, solvent, and template agents, etc.[7] Thus, design and synthesis of the preferred structures are still a fundamental scientific challenge.

The past decades have seen significant progress to design and construct PMOFs by reasonable selection of the organic linkers and the secondary building units (SBUs) before the assemble process. Generally, the organic linkers are confined to presynthesized or commercially available ligands; however, in situ ligand synthesis, as one of the most powerful tactics to form unexpected ligands, is of increasing interest. To date, various in situ reactions have been reported, such as hydroxylation, alkylation, decarboxylation, hydrolysis, tetrazole and triazole formation, acylation, and cis–trans isomerization, etc.[8] The unexpected ligands formed during the in situ reaction can be incorporated into the resultant novel coordination polymers. Among them, in situ decarboxylic reaction is only a simple change of functional group. Currently, in situ decarboxylic reaction mainly focuses on the multicarboxylic acid ligands containing N-donors.[9] The decarboxylation of carboxylate ligands without N-donors has been less studied. Therefore, the study on decarboxylation is of great significance for the construction of unexpected novel coordination polymers.

Furthermore, C_3-symmetric tritopic organic linkers have gained huge interest due to the diversity for constructing 3D porous materials. Numerous PMOFs with high surface areas and large pore sizes were constructed by employment of a C_3-symmetric ligand. As one of the most typical examples, MOF-210 $[(Zn_4O)_3(BTE)_4(BPDC)_3$; BTE: 4,4′,4″-(benzene-1,3,5-triyl-tris(ethyne-2,1-diyl))tribenzoate; BPDC: biphenyl-4,4′-dicarboxylate], exhibits the highest total H_2 storage capacity and the lowest crystal density for reported MOFs.[10] In addition, some famous MOFs, such as HKUST-1, MOF-177, and MOF-200, are all constructed with C_3-symmetric ligands, and all show high surface areas and large pore sizes.[11] Our group has also

Received: July 25, 2014

   dx.doi.org/10.1021/ic501801f | *Inorg. Chem.* XXXX, XXX, XXX–XXX

designed and synthesized a class of trinodal carboxylate ligands, and various open crystalline frameworks have been gained and studied on the applications in gas storage and catalysis.[12] In this work, we selected and synthesized a triarylboron-functionalized C_3-symmetric ligand, tris(p-carboxylic acid)tridurylborane (H_3L^1, Scheme 1), mainly considering its following character-

Scheme 1. H_3L^1 and H_2L^2 Involved in This Work

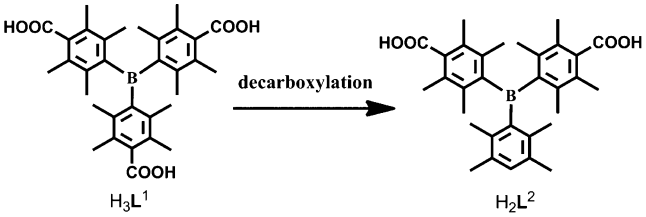

H_3L^1 H_2L^2

istics: (i) the lewis acidic triarylboryl group that is luminescent and capable of binding to and sensing small guest molecules,[13] and (ii) the incorporation of hindrance groups ($-CH_3$) into the ligand, which can effectively control interpenetration.[14] Although a few instances of triarylboron-functionalized metal–organic frameworks (B-MOF) have been documented,[15] reports on the gas adsorption and decarboxylic reaction are still rare.

Herein, we report two new 3D triarylboron-functionalized, noninterpenetrating MOFs, $[Cd_3(L^1)_2(DMA)_2]\cdot DMA$ (**1**) and $[Zn_3(L^2)_3(H_2O)_2]\cdot 5H_2O\cdot 2EtOH$ (**2**). Interestingly, when complex **2** was prepared with H_3L^1 in mixed solvent (H_2O/EtOH = 1/4), H_3L^1 was changed into 4,4′-((2,3,5,6-tetramethylphenyl)boranediyl)bis(2,3,5,6-tetramethylbenzoic acid) (H_2L^2) due to the in situ decarboxylic reaction (Scheme 1). Such similar reactions have also been reported in previous literature.[16]

EXPERIMENTAL SECTION

Materials and General Methods. The H_3L^1 ligand was synthesized according to the previous literatures.[15] All of the starting materials and solvents were purchased from commercial vendors and used without further purification. IR spectra were collected on a Bruker VERTEX-70 spectrometer within the 4000–400 cm^{-1} region. Thermogravimetric analysis (TGA) experiments were carried out on a PerkinElmer TGA 7 instrument under a static N_2 atmosphere with a heating rate 10 °C min^{-1} at the range 30–800 °C. Elemental analyses (C, H, and N) were performed using a PerkinElmer 240 elemental analyzer. The powder X-ray diffraction data were obtained on a Bruker AXS D8 Advance. Photoluminescence spectra were recorded with a Hitachi F-4500 fluorescence spectrophotometer. Gas sorption experiments were carried out on the surface area analyzer ASAP-2020.

Synthesis of Complex 1 $[Cd_3(L^1)_2(DMA)_2]\cdot DMA$. $Cd(NO_3)_2\cdot 4H_2O$ (5.0 mg, 0.016 mmol), H_3L^1 (2.0 mg, 0.0053 mmol), and DMA (1 mL) were heated to 120 °C for 3000 min in a sealed tube. The colorless crystalline blocks formed on the wall of the glass tube were collected by filtration, washed with DMA and EtOH, and dried in air (yield: 25%, based on cadmium). Anal. Calcd (Found) for **1**: C, 57.19 (57.21); H, 6.48 (6.55); N, 3.88 (3.84)%. IR peaks (KBr, cm^{-1}): 3512 (m), 2933 (m), 1623 (s), 1542 (s), 1417 (s), 1275 (m), 1097 (w), 1035 (w), 873 (m), 668 (m).

Synthesis of Complex 2 $[Zn_3(L^2)_3(H_2O)_2]\cdot 5H_2O\cdot 2EtOH$. $Zn(NO_3)_2\cdot 6H_2O$ (20 mg, 0.068 mmol), H_3L^1 (20 mg, 0.053 mmol), and 5 mL EtOH and H_2O (v/v = 4/1) were heated to 120 °C for 3000 min in a 20 mL vial. The colorless, block-shaped crystals were obtained and washed with EtOH (yield: 30%, based on zinc). Anal. Calcd (Found) for **2**: C, 63.19 (63.35), H, 7.00 (7.12)%. IR peaks (KBr, cm^{-1}): 3442 (m), 2924 (m), 1657 (s), 1551 (s), 1417 (s), 1275 (s), 1096 (w), 1043 (w), 865 (w), 632 (w).

X-ray Structural Studies. Crystals of **1** and **2** with appropriate dimensions were quickly mounted on a glass fiber under an optical microscope. Their X-ray diffraction data were collected on a Agilent Xcalibur Eos Gemini diffractometer with Mo Kα (λ = 0.710 73 Å) at 293 K and Cu Kα radiation (λ = 1.541 78 Å) at 150 K, respectively. Absorption corrections were applied using the multiscan method. All structures were solved by direct methods and refined by full-matrix least-squares on F^2 using *SHELXL-97*.[17] All non-hydrogen atoms were located from iterative examination of difference F-maps and refined with anisotropic thermal parameters on F^2. The organic hydrogen atoms were placed in calculated positions and refined as riding atoms with isotropic displacement parameters 1.2–1.5 times U_{eq} of the attached atoms. The free solvent molecules in **1** and **2** are highly disordered, and no satisfactory disorder model could be achieved. The *PLATON/SQUEEZE* routine was used to remove scattering from the disordered solvent molecules.[18] Pertinent crystallographic data collection and refinement parameters are collected in Table 1.

Table 1. Crystal Data for Complexes 1 and 2

	1	2
formula	$C_{82}H_{108}B_2Cd_3N_4O_{16}$	$C_{96}H_{111}B_3Zn_3O_{14}$
M_r	1764.54	1717.39
cryst syst	monoclinic	cubic
space group	$P2_1/c$	$Ia\bar{3}d$
a (Å)	14.9156(7)	37.0156(11)
b (Å)	15.0624(8)	37.0156(11)
c (Å)	28.7668(11)	37.0156(11)
α (deg)	90.00	90.00
β deg)	117.561(3)	90.00
γ (deg)	90.00	90.00
Z	2	16
V (Å^3)	5729.5(5)	50 717(3)
D_c (g cm^{-3})	1.023	0.900
μ (mm^{-1})	0.599	1.008
F (000)	1820.0	14464.0
no. unique reflns	20 600	17 102
no. obsd reflns [$I > 2\sigma(I)$]	10 078	4026
params	500	183
GOF	1.077	1.006
final R indices [$I > 2\sigma(I)$][a,b]	R1 = 0.0680	R1 = 0.0862
	wR2 = 0.1782	wR2 = 0.2178
R indices (all data)	R1= 0.1136	R1 = 0.1618
	wR2 = 0.1953	wR2 = 0.2478
Δ_ρ (e Å^{-3})	1.35 and −1.39	0.30 and −0.46

[a] $R1 = \Sigma||F_o| - |F_c||/\Sigma|F_o|$. [b] $wR2 = [\Sigma w(F_o^2 - F_c^2)^2/\Sigma w(F_o^2)^2]^{0.5}$.

Selected bond distances and angles are given in Supporting Information Table S1. Crystallographic data have been deposited at the Cambridge Crystallographic Data Center (CCDC: 1010289, 1010290). These data can be obtained from the Cambridge Crystallographic Data Center, 12, Union Road, Cambridge CB21EZ, U.K.

RESULTS AND DISCUSSION

Synthesis. The H_3L^1 ligand was synthesized by treating tris(pbromoduryl)borane with *tert*-butyllithium and CO_2 at 78 K according to the literature and was characterized by ^1H NMR.[15] Complexes **1** and **2** were obtained by heating a mixture of H_3L^1 and $Cd(NO_3)_2\cdot 4H_2O$ or $Zn(NO_3)_2\cdot 6H_2O$ at 120 °C for 3000 min by solvothermal reactions. During the formation of complex **2**, in situ decarboxylic reaction occurred and H_3L^1 was transformed into H_2L^2. At the same temperature and pressure, when the solvent were changed, complex **2** can not be obtained. Thus, the selection of solvent for the in situ

dx.doi.org/10.1021/ic501801f | Inorg. Chem. XXXX, XXX, XXX–XXX

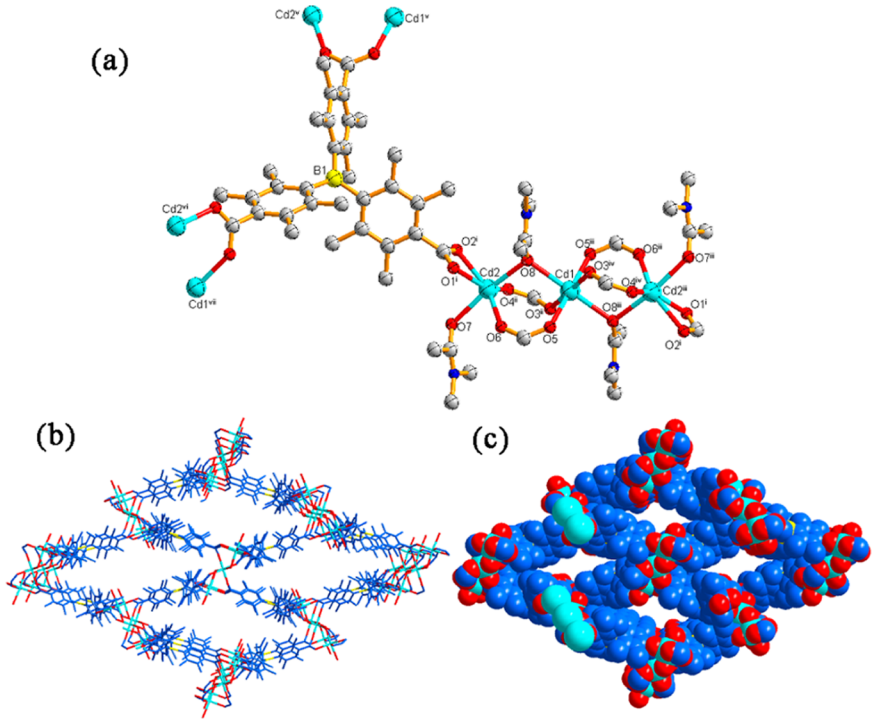

Figure 1. (a) Coordination environment of Cd(II) ions in **1** and the linkage mode of $H_3\mathbf{L}^1$. (b) Projection view of 3D open framework along the *a* axis, showing the rhombic channels. (c) Space filling representation of the 3D porous framework (symmetry codes: (i) $x + 1, y, z$; (ii) $x + {}^1/_2, -y + {}^3/_2, z + {}^1/_2$; (iii) $-x + 2, -y + 2, -z + 1$; (iv) $-x + {}^3/_2, y + {}^1/_2, -z + {}^1/_2$; (v) $x - 1, y, z$; (vi) $x - {}^1/_2, -y + {}^3/_2, z - {}^1/_2$; (vii) $-x + {}^3/_2, y - {}^1/_2, -z + {}^1/_2$).

reaction is important. The structures of **1** and **2** were confirmed by single crystal X-ray analysis, elemental analysis, IR spectrum, and X-ray powder diffraction.

Crystal Structures of 1 and 2. X-ray single crystal diffraction analysis reveals that complex **1** crystallizes in the monoclinic space group $P2_1/n$ and possesses a neutral 3D open framework based on trinuclear cadmium SBUs. The asymmetric unit contains half Cd1 ion, one dependent Cd2 ion, one $\mathbf{L}^1$ ligand, and two coordinated DMA molecules. Figure 1a shows the coordination environments of two Cd(II) atoms. Cd1 is six-coordinated in an octahedron geometry, completed by four oxygen atoms from different $\mathbf{L}^1$ ligands and two oxygen atoms from coordinated DMA molecules. Cd2 also shows a slightly distorted octahedron geometry, but it is coordinated by four oxygen atoms from three $\mathbf{L}^1$ ligands and two oxygen atoms from coordinated DMA molecules. The Cd−O bond average distances are 2.263 and 2.272 Å for Cd1 and Cd2, respectively, which are consistent with the previously reported literatures.[19] One Cd1 and two Cd2 ions are engaged by four carboxylate groups and two bridging DMA molecules to form a trinuclear SBU with a Cd1−Cd2 distance of 3.729 Å. During the reaction, three carboxylate groups of the ligand are all deprotonated and adopt two types of coordination modes: bridging (μ^2-η^1:η^1) and chelating (η^2). Each ligand connects three trinuclear SBUs.

The trinuclear hourglass SBUs are connected by the $\mathbf{L}^1$ organic linkers to generate 3D open framework with 1D rhombic channels along the *a* direction. The dimensions of the channels are about 25.5 × 7.5 Å^2 (Figure 1b,c). The void space accounts for approximately 30.3%,[20] which is occupied by disordered solvent molecules. The topological analysis of complex **1** by *TOPOs* software reveals that the overall topology is a (3, 6)-connected network with the point symbols (4.6^2) and ($4^2.6^{10}.8^3$) and belongs to a *rtl* topology (Figure 2).[21]

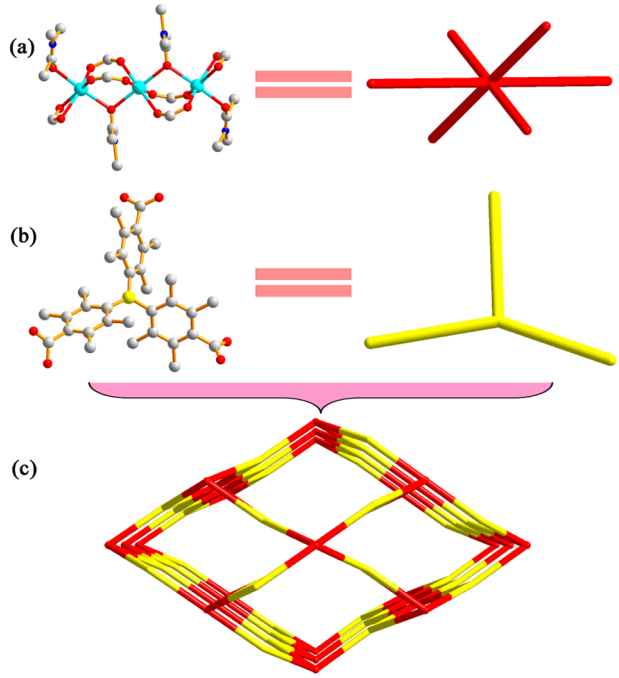

Figure 2. Schematic representations of a simplified 3D network for **1** with *rtl* topology (c) containing 6-connected nodes (a) and 3-connected nodes (b).

A single crystal X-ray diffraction study reveals that **2** is a neutral 3D PMOF based on a hourglass SBU. Complex **2** crystallizes in the cubic space group $Ia\bar{3}d$. The asymmetric unit contains one-sixth Zn1 ion, one-third Zn2 ion, half $\mathbf{L}^2$ ligand, and one-third coordinated H_2O molecule. Both carboxylate

dx.doi.org/10.1021/ic501801f | *Inorg. Chem.* XXXX, XXX, XXX−XXX

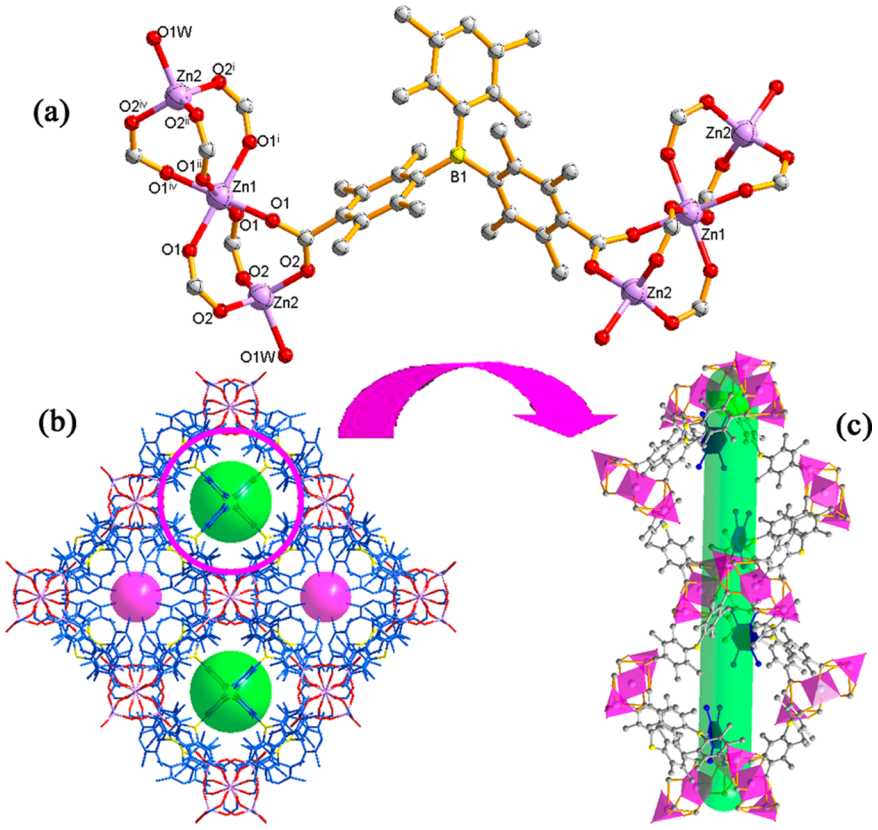

Figure 3. (a) Coordination environment of Zn (II) ions in **2** and the linkage mode of H_2L^2. (b) 3D structure of **2** along the *a* axis. The channels are highlighted by green spheres and rose-red spheres. (c) View of the channel along the *b* axis with four phenyl groups highlighted by blue plane in the channel (symmetry codes: (i) $-y + 1, -z + 1, -x + 1$; (ii) $-z + 1, -x + 1, -y + 1$; (iii) z, x, y; (iv) $-x + 1, -y + 1, -z + 1$).

groups of the ligand are deprotonated during the reaction, and each carboxylate group bridges two Zn (II) ions. As shown in Figure 3a, one Zn1 and two Zn2 ions are linked by six carboxylate groups to form a trinuclear hourglass SBU with a Zn1−Zn2 distance of 3.692 Å, which is similar to that found in complex **1**. Zn1 is six-coordinated in an octahedron geometry by six oxygen atoms from different L^2 ligands, whereas Zn2 is four-coordinated in a slightly distorted tetrahedron geometry by three oxygen atoms from L^2 ligands and one oxygen atom from the coordinated water molecule. The average Zn−O distances are 2.078 and 1.963 Å for Zn1 and Zn2, respectively. Each L^2 ligand connects two trinuclear hourglass SBUs, and every SBU attaches to six L^2 ligands to generate a 3D porous structure (Figure 3b). As shown in Figure 3b, complex **2** contains two kinds of cavities: one is highlighted by green sphere with the diameter of 9.8 Å; the other is highlighted by red sphere with the diameter of 4.5 Å. The cavities highlighted by green sphere are filled by some phenyl groups, while these phenyl groups are not in a plane, leading to a curved channel (Figure 3c). Thus, the void volume is larger than that shown in Figure 3b, which may be beneficial to the gas sorption properties of **2**. The void volume calculated by *PLATON* is 32.8%, which is occupied by disordered solvent molecules.[20] To further study the nature of the intricate framework, its topology was analyzed with free computer program *TOPOs*.[21] The L^2 ligand and the trinuclear hourglass SBUs can be taken as a linear linker and a 6-connected node, respectively, giving rise to a 6-connected net with the point symbol ($4^6.6^9$), which belongs to a *bcs* topology (Figure 4).

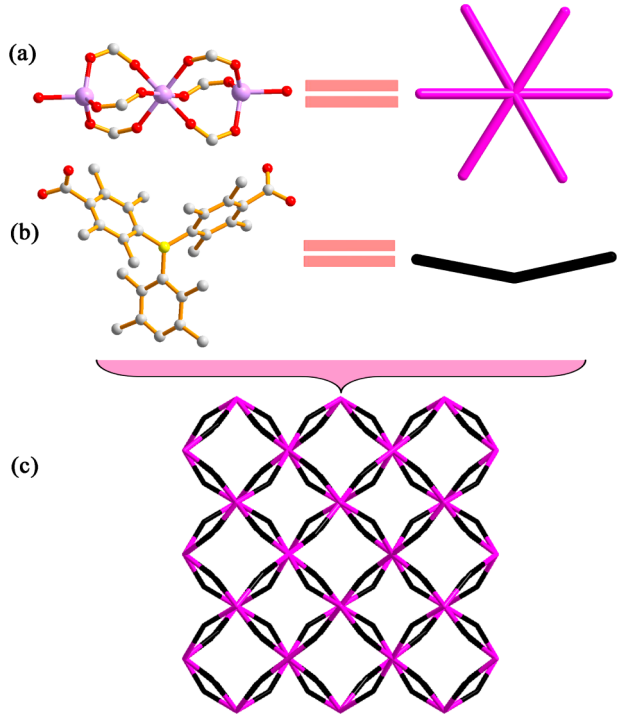

Figure 4. Schematic representations of a simplified 3D network for **2** with 6-c topology (c) containing 6-connected nodes (a) and 2-connected nodes (b).

dx.doi.org/10.1021/ic501801f | *Inorg. Chem.* XXXX, XXX, XXX−XXX

Thermal Analyses, IR Spectra, and X-ray Powder Diffraction Analyses. The thermal behaviors of complexes **1** and **2** were investigated under a dry nitrogen atmosphere from 25 to 800 °C and the TG curves were presented in Supporting Information Figure S1. Complex **1** shows no weight loss between 25 to 80 °C, followed by a weight loss of 24.23% from 80 to 220 °C due to the loss of four coordinated and one lattice DMA molecules (calcd: 24.11%). Beyond 300 °C, a rapid weight loss is observed, indicating the decomposition of complex **1** and the formation of CdO as the main residue. The TG curve of **2** shows a weight loss of 11.64% from 30 to 224 °C corresponding to the loss of lattice and coordinated H_2O molecules (calcd: 11.48%). Then, the complex starts to decompose. The IR spectrum and X-ray powder diffraction for complexes **1** and **2** have also been measured to confirm their structure and the phase purity, which are shown in Supporting Information Figures S2 and S3, respectively.

Luminescent Properties. Luminescent complexes have attracted intense interest for their potential applications in chemical sensors, electroluminescent display, photochemistry, and so on.[22] Herein, the photoluminescent properties of **1**, **2**, and $H_3\mathbf{L}^1$ were investigated intensively at room temperature. As shown in Supporting Information Figure S4, free ligand $H_3\mathbf{L}^1$ displays a purple-blue fluorescence at 396 nm (λ_{ex} = 300 nm), which originates from the $\pi^*\cdots\pi$ transition of the p electrons of aromatic rings.[23] The similar luminescent property has also been reported for other triarylboron-containing compounds.[15] Complex **1** exhibits luminescent emission band at 406 nm (λ_{ex} = 300 nm). To compare with $H_3\mathbf{L}^1$, it has a red-shifted (Δ = 10 nm) photoluminescence due to the metal-to-ligand charge transfer transitions. Meanwhile, complex **2** shows photoluminescence with emission maxima at 400 nm (λ_{ex} = 300 nm). It is obvious that the emission bands for complexes **1** and **2** resemble those of triarylboron-containing ligands, so the emissions of **1** and **2** are possible attributed to the ligands $\pi^*\cdots\pi$ transitions modified by metal coordination.

Gas Sorption of Complexes 1 and 2. To investigate the permanent porosities of **1** and **2**, the gas isotherms were measured for N_2 at 77 K. The as-synthesized **1** and **2** were guest-exchanged with dry methanol and dichloromethane, respectively, followed by activation at 60 °C under high vacuum for 3 h to get the activated **1** and **2**. Figure 5 shows the N_2 sorption isotherms at 77 K for complexes **1** and **2**. The Langmuir surface area of **1** is 9.6895 $m^2\ g^{-1}$. The uptake of N_2 is only 6.0 $cm^3\ g^{-1}$ at 1 bar. The measured pore volume from N_2 sorption is 0.007 06 $cm^3\ g^{-1}$, which is much lower than that estimated from the single crystal structure (cald: 0.296 $cm^3\ g^{-1}$),[24] indicating that the host framework is easy to collapse after removing solvents from the crystalline samples. Meanwhile, the N_2 adsorption isotherm shows a type-II sorption behavior, which further demonstrates a collapse structure of desolvated **1**. Moreover, desolvated **2** displays typical type-I adsorption isotherms for N_2, which suggests the retention of the microporous structure after removal of guest molecules. It is possible that the SBU with four coordinated DMA molecules in **1** is more unstable than the SBU with two coordinated H_2O molecules in **2**. As shown in Figure 5, the isotherm for **2** has an abrupt slope from 0.01 to 0.1 bar, which indicates that the pores are filled in sequence as the increasing of pressure from 0.01 to 0.1 bar. Subsequently, the N_2 uptake capacity of **2** increases slightly and reaches a platform (185 $cm^3\ g^{-1}$) at 1 bar. The BET and Langmuir surface areas are calculated to be 680.2 $m^2\ g^{-1}$ and 771.3 $m^2\ g^{-1}$, respectively. The measured pore volume is 0.2859 $cm^3\ g^{-1}$. The parameters of **2** are much larger than those of **1**. The mean pore size distribution is about 12.7 Å for complex **2** (Supporting Information Figure S5). Remarkably, the uptake of N_2 for **2** is higher than that reported for the Zn^{II}B-MOF compound (~140 $cm^3\ g^{-1}$), and the pore volume of 0.2859 $cm^3\ g^{-1}$ is larger than that for the Zn^{II}B-MOF compound (0.21 $cm^3\ g^{-1}$),[15c] which may derive from the observation that shorter linker and hindrance groups avoid interpenetration and lead to a larger pore volume to compare with $\mathbf{L}^1$ ligand (tris(2′,3′,5′,6′-tetramethylbiphenyl-4-carboxylic acid)borane).

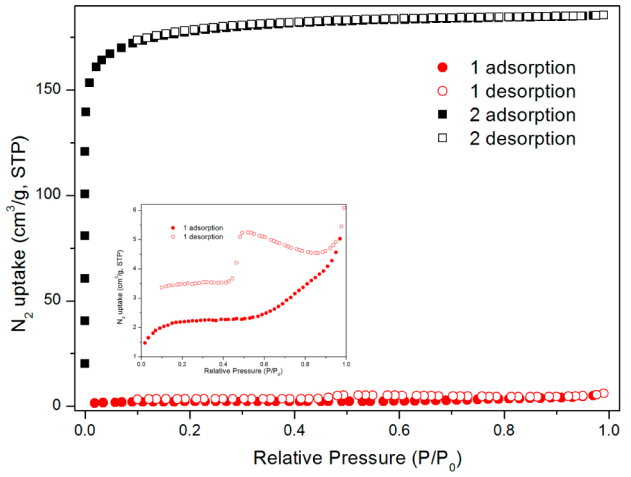

Figure 5. N_2 sorption isotherms for **1** and **2** at 77 K. The enlarged view of the N_2 sorption isotherm for **1** is shown in the inset.

In addition, low-pressure Ar, H_2, CO_2, and CH_4 sorption experiments for complex **2** were measured at a variety of temperatures. Their sorption isotherms are exhibited in Figure 6. The uptake of Ar for **2** is 220 $cm^3\ g^{-1}$, which is also higher than that of the Zn^{II}B-MOF compound (~160 $cm^3\ g^{-1}$).[15c] Under the conditions of 1 bar and 77 K, desolvated **2** exhibits the H_2 uptake capacity of 115 $cm^3\ g^{-1}$ (1.02 wt %). The value surpasses that of the favorable zeolite ZSM-5 (0.7 wt %) and is close to those of some reported MOFs at the same condition.[25] The gas isosteric heat of adsorption (Q_{st}) can be calculated by fitting the gas adsorption isotherms at different temperature to a virial-type expression.[26] By this method, the Q_{st} for H_2 was obtained by fitting the H_2 adsorption isotherms at 77 and 87 K and had the estimated value of 7.0 kJ mol^{-1} (Supporting Information Figure S6a). The sorption isotherms for CO_2 reveal that **2** stores CO_2 up to 49.3 $cm^3\ g^{-1}$ (9.6 wt %) at 273 K and 1 atm, and 33.4 $cm^3\ g^{-1}$ (6.5 wt %) at 295 K and 1 atm. The CO_2 sorption capacity of **2** is higher than those for the favorable zeolites ZIF-79, ZIF-70, and ZIF-100, and is close to those for some reported MOFs, such as MOF-253, YO-MOF, and CPL-2, etc.[27] Complex **2** adsorbs 12.2 $cm^3\ g^{-1}$ of CH_4 at 273 K and 1 atm, and 8.87 $cm^3\ g^{-1}$ of CH_4 at 295 K and 1 atm. The Q_{st} for CO_2 and CH_4 at low coverage can be calculated by fitting the gas adsorption isotherms at 273 and 295 K. The values for CO_2 and CH_4 are 17.7 and 9.6 kJ mol^{-1}, respectively (Supporting Information Figure S6b,c).

CONCLUSIONS

We have successfully synthesized two 3D noninterpenetrating MOFs (**1** and **2**) built from trinuclear SBUs and organoboron carboxylate ligands. Complex **1** exhibits a (3, 6)-connected

dx.doi.org/10.1021/ic501801f | Inorg. Chem. XXXX, XXX, XXX−XXX

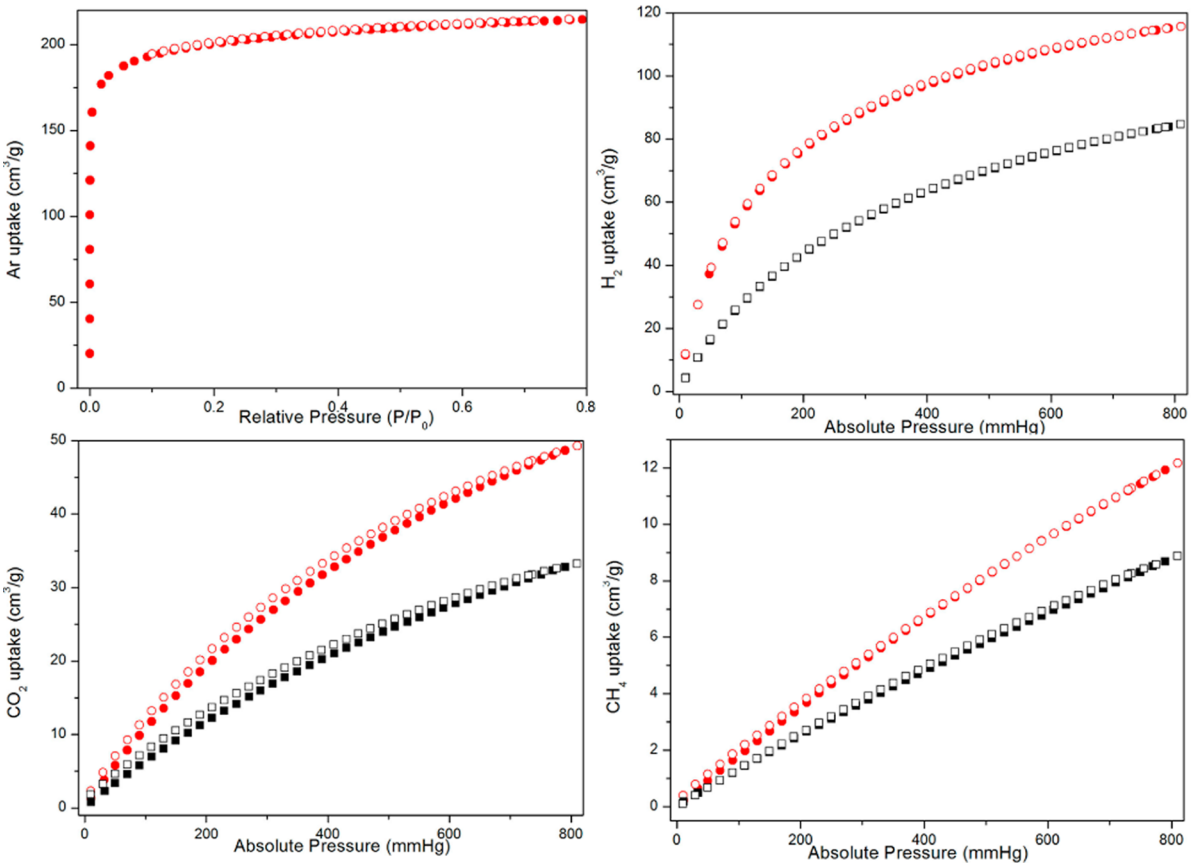

Figure 6. Ar, H_2, CO_2, and CH_4 sorption isotherms for **2**: Ar, red 77 K; H_2, red 77 K, black 87 K; CO_2, red 273 K, black 295 K; CH_4, red 273 K, black 295 K.

topological network based on a Cd_3 cluster and a trinodal organic linker, and **2** shows a 6-connected topology due to the in situ decarboxylic reaction of $H_3\mathbf{L}^1$. Both MOFs exhibit blue fluorescence. Complex **1** with large rhombic channels is easy to collapse after removal of guest molecules, while complex **2** with small channels exhibits permanent porosity with Langmuir surface area of 771.3 $m^2\ g^{-1}$. Our results presented here further indicate that the stable SBU is crucial to the assembly of porous MOF with permanent porosity. Furthermore, the in situ reaction such as decarboxylation is still a facile strategy on the construction of MOFs with unexpected structure.

■ ASSOCIATED CONTENT

Ⓢ Supporting Information

Selected bond lengths and bond angles (Table S1), TGA curves (Figure S1), IR curves (Figure S2), PXRD patterns (Figure S3), solid-state emission spectra (Figure S4), the pore size distribution of **2** (Figure S5), and the gas isosteric heat of adsorption for **2** (Figure S6). Crystallographic information in CIF format. This material is available free of charge via the Internet at http://pubs.acs.org.

■ AUTHOR INFORMATION

Corresponding Authors

*E-mail: fndai@upc.edu.cn.
*E-mail: dfsun@sdu.edu.cn.

Notes

The authors declare no competing financial interest.

■ ACKNOWLEDGMENTS

This work was supported by the NSFC (Grants 21271117, 21371179), NCET-11-0309, the Shandong Natural Science Fund for Distinguished Young Scholars (JQ201003), the China Postdoctoral Science Foundation (2014T70665), and the Fundamental Research Funds for the Central Universities (13CX05010A, 13CX02006A).

■ REFERENCES

(1) (a) Murray, L. J.; Dincaă, M.; Long, J. R. *Chem. Soc. Rev.* **2009**, *38*, 1294−1314. (b) Suh, M. P.; Park, H. J.; Prasad, T. K.; Lim, D. W. *Chem. Rev.* **2012**, *112*, 782−835. (c) Zhou, H. C.; Long, J. R.; Yaghi, O. M. *Chem. Rev.* **2012**, *112*, 673−674. (d) Sumida, K.; Rogow, D. L.; Mason, J. A.; McDonald, T. M.; Bloch, E. D.; Herm, Z. R.; Bae, T. H.; Long, J. R. *Chem. Rev.* **2012**, *112*, 724−781.

(2) (a) Ma, L.; Falkowski, J. M.; Abney, C.; Lin, W. *Nat. Chem.* **2010**, *2*, 838−846. (b) Ameloot, R.; Vermoortele, F.; Vanhove, W.; Roeffaers, M. B. J.; Sels, B. F.; Vos, D. E. D. *Nat. Chem.* **2011**, *3*, 382−387.

(3) (a) Cui, Y. J.; Yue, Y. F.; Qian, G. D.; Chen, B. L. *Chem. Rev.* **2012**, *112*, 1126−1162. (b) Cui, Y. J.; Xu, H.; Yue, Y. F.; Guo, Z. Y.; Yu, J. C.; Chen, Z. X.; Gao, J. K.; Yang, Y.; Qian, G. D.; Chen, B. L. *J. Am. Chem. Soc.* **2012**, *134*, 3979−3982. (c) Wei, Z.; Gu, Z.-Y.; Arvapally, R. K.; Chen, Y.-P.; McDougald, R. N., Jr.; Lvy, J. F.; Yakovenko, A. A.; Feng, D.; Omary, M. A.; Zhou, H. C. *J. Am. Chem. Soc.* **2014**, *136*, 8269−8276.

(4) (a) He, Y. B.; Zhou, W.; Krishna, R.; Chen, B. L. *Chem. Commun.* **2012**, *48*, 11813−11831. (b) Narayan, T. C.; Miyakai, T.; Seki, S.; Dincă, M. *J. Am. Chem. Soc.* **2012**, *134*, 12932−12935. (c) Yoon, M.; Suh, K.; Natarajan, S.; Kim, K. *Angew. Chem., Int. Ed.* **2013**, *52*, 2688−2700.

dx.doi.org/10.1021/ic501801f | *Inorg. Chem.* XXXX, XXX, XXX−XXX

(5) (a) Taylor-Pashow, K. M. L.; Rocca, J. D.; Xie, Z. G.; Tran, S.; Lin, W. B. *J. Am. Chem. Soc.* **2009**, *131*, 14261−14263. (b) Ke, F.; Yuan, Y. P.; Qiu, L. G.; Shen, Y. H.; Xie, A. J.; Zhu, J. F.; Tian, X. Y.; Zhang, L. D. *J. Mater. Chem.* **2011**, *21*, 3843−3848.
(6) (a) Horcajada, P.; Gref, R.; Baati, T.; Allan, P. K.; Maurin, G.; Couvreur, P.; Férey, G.; Morris, R. E.; Serre, C. *Chem. Rev.* **2012**, *112*, 1232−1268. (b) Fei, H.; Shin, J.; Meng, Y. S.; adelhardt, M.; Sutter, J.; Meyer, K.; Cohen, S. M. *J. Am. Chem. Soc.* **2014**, *136*, 4965−4973.
(7) (a) Gao, J. K.; Ye, K. Q.; Yang, L.; Xiong, W. W.; Ye, L.; Wang, Y.; Zhang, Q. *Inorg. Chem.* **2014**, *53*, 691−693. (b) He, Y. P.; Tan, Y. X.; Zhang, J. *Inorg. Chem.* **2013**, *52*, 12758−12762. (c) Cui, P.; Wu, J.; Zhao, X.; Sun, D.; Zhang, L.; Guo, J.; Sun, D. *Cryst. Growth Des.* **2011**, *11*, 5182−5187. (d) Chen, L.; Mowat, J. P. S.; Fairen-Jimenez, D.; Morrison, C. A.; Thompson, S. P.; Wright, P. A.; Duren, T. *J. Am. Chem. Soc.* **2013**, *135*, 15763−15773. (e) Santra, A.; Bharadwaj, P. K. *Cryst. Growth Des.* **2014**, *14*, 1476−1485. (f) Wang, X. L.; Qin, C.; Wang, E. B.; Li, Y.-G.; Su, Z.-M.; Xu, L.; Carlucci, L. *Angew. Chem., Int. Ed.* **2005**, *44*, 5824−5827. (g) Zhu, Q. L.; Xu, Q. *Chem. Soc. Rev.* **2014**, *43*, 5468−5512. (h) Lu, W.; Wei, Z.; Gu, Z. Y.; Liu, T. F.; Park, J.; Park, J.; Tian, J.; Zhang, M.; Zhang, Q.; Gentle, T.; Bosch, M.; Zhou, H.-C. *Chem. Soc. Rev.* **2014**, *43*, 5561−5593.
(8) (a) Liu, J. L.; Chen, Y. C.; Li, Q. W.; Gomez-Coca, S.; Aravena, D.; Ruiz, E.; Lin, W. Q.; Leng, J. D.; Tong, M. L. *Chem. Commun.* **2013**, *49*, 6549−6551. (b) Cheng, J. K.; Yao, Y. G.; Zhang, J.; Li, Z. J.; Cai, Z. W.; Zhang, X. Y.; Chen, Z. N.; Chen, Y. B.; Kang, Y.; Qin, Y. Y.; Wen, Y. H. *J. Am. Chem. Soc.* **2004**, *126*, 7796−7797. (c) Zhong, D. C.; Lu, W. G.; Jiang, L.; Feng, X. L.; Lu, T. B. *Cryst. Growth Des.* **2010**, *10*, 739−746. (d) Li, J. R.; Yu, Q.; Tao, Y.; Bu, X. H.; Ribas, J.; Batten, S. R. *Chem. Commun.* **2007**, *22*, 2290−2292. (e) Xiong, R. G.; Xue, X.; Zhao, H.; You, X. Z.; Abrahams, B. F.; Xue, Z. L. *Angew. Chem., Int. Ed.* **2002**, *41*, 3800−3803. (f) Hu, X. X.; Xu, J. Q.; Cheng, P.; Chen, X. Y.; Cui, X. B.; Song, J. F.; Yang, G. D.; Wang, T. G. *Inorg. Chem.* **2004**, *43*, 2261−2266. (g) Knaust, J. M.; Keller, S. W. *Inorg. Chem.* **2002**, *41*, 5650−5652.
(9) (a) Sun, Y. Q.; Zhang, J.; Yang, G. Y. *Chem. Commun.* **2006**, 1947−1949. (b) Liao, S. Y.; Gu, W.; Yang, L. Y.; Li, T. H.; Tian, J. L.; Wang, L.; Zhang, M.; Liu, X. *Cryst. Growth Des.* **2012**, *12*, 3927−3936. (c) Tseng, T. W.; Luo, T. T.; Chen, S. Y.; Su, C. C.; Chi, K. M.; Lu, K. L. *Cryst. Growth Des.* **2013**, *13*, 510−517.
(10) Furukawa, H.; Ko, N.; Go, Y. B.; Aratani, N.; Choi, S. B.; Choi, E.; Yazaydin, A. O.; Snurr, R. Q.; O'Keeffe, M.; Kim, J.; Yaghi, O. M. *Science* **2010**, *329*, 424−428.
(11) (a) Chui, S. S. Y.; Lo, S. M. F.; Charmant, J. P. H.; Orpen, A. G.; Williams, L. D. *Science* **1999**, *19*, 1148−1150. (b) Chae, H. K.; Siberio-Pérez, D. Y.; Kim, J.; Go, Y. B.; Eddaoudi, M.; Matzger, A. J.; O'Keeffe, M.; Yaghi, O. M. *Nature* **2004**, *427*, 523−527. (c) Sun, D.; Collins, D. J.; Ke, Y.; Zuo, J. L.; Zhou, H. C. *Chem.—Eur. J.* **2006**, *12*, 3768−3776.
(12) (a) Ma, H. Q.; Sun, D.; Zhang, L. L.; Wang, R. M.; Blatov, V. A.; Guo, J.; Sun, D. F. *Inorg. Chem.* **2013**, *52*, 10732−10734. (b) Zhao, X. L.; He, H. Y.; Dai, F. N.; Sun, D. F.; Ke, Y. X. *Inorg. Chem.* **2010**, *49*, 8650−8652. (c) Zhao, X. L.; Dou, J. M.; Sun, D.; Cui, P. P.; Sun, D. F.; Wu, Q. Y. *Dalton Trans.* **2012**, *41*, 1928−1930.
(13) (a) Kubo, Y.; Yamamoto, M.; Ikeda, M.; Takeuchi, M.; Shinkai, S.; Yamaguchi, S.; Tamao, K. *Angew. Chem., Int. Ed.* **2003**, *42*, 2036−2040. (b) Sun, Y.; Ross, N.; Zhao, S.-B.; Huszarik, K.; Jia, W.-L.; Wang, R.-Y.; Macartney, D.; Wang, S. *J. Am. Chem. Soc.* **2007**, *129*, 7510−7511. (c) Wade, C. R.; Broomsgrove, A. E. J.; Aldridge, S.; Gabbaï, F. P. *Chem. Rev.* **2010**, *110*, 3958−3984.
(14) He, H.; Yuan, D.; Ma, H.; Sun, D.; Zhang, G.; Zhou, H. C. *Inorg. Chem.* **2010**, *49*, 7605−7607.
(15) (a) Liu, Y.; Xu, X.; Zheng, F. K.; Cui, Y. *Angew. Chem., Int. Ed.* **2008**, *120*, 24614−4617. (b) Liu, Y.; Xuan, W. M.; Zhang, H.; Cui, Y. *Inorg. Chem.* **2009**, *48*, 10018−10023. (c) Blight, B. A.; Guillet-Nicolas, R.; Kleitz, F.; Wang, R. Y.; Wang, S. *Inorg. Chem.* **2013**, *52*, 1673−1675. (d) Liu, Y.; Cui, Y. *Inorg. Chem.* **2013**, *52*, 10286−10291. (e) Varlan, M.; Blight, B. A.; Wang, S. *Chem. Commun.* **2012**, *48*, 12059−12061. (f) Blight, B. A.; Stewart, A. F.; Wang, N.; Lu, J. S.; Wang, S. *Inorg. Chem.* **2012**, *51*, 778−780. (g) Zhang, J.; Chen, S. M.; Bu, X. H. *Dalton Trans.* **2010**, *39*, 2487−2489. (h) Zhang, H. X.; Wang, F.; Yang, H.; Tan, Y. X.; Zhang, J.; Bu, X. H. *J. Am. Chem. Soc.* **2011**, *133*, 11884−11887.
(16) (a) Cai, S. L.; Zheng, S. R.; Tan, J. B.; Pan, M.; Fan, J.; Zhang, W. G. *CrystEngComm* **2011**, *13*, 6345−6348. (b) Nadeem, M. A.; Bhadbhade, M.; Bircher, R.; Stride, J. A. *Cryst. Growth Des.* **2010**, *10*, 4060−4067. (c) Cheng, Y. F.; Lu, X. M.; Wang, G. *Dalton Trans.* **2014**, *14*, 5357−5363.
(17) Sheldrick, G. M. *SHELXL-97, Program for X-ray Crystal Structure Refinement*; University of Gottingen: Gottingen, Germany, 1997.
(18) Spek, A. L. *Implemented as the PLATON Procedure, a Multipurpose Crystallographic Tool*; Utrecht University: Utrecht, The Netherlands, 1998.
(19) (a) Su, Z.; Bai, Z.-S.; Fan, J.; Xu, J.; Sun, W. Y. *Cryst. Growth Des.* **2009**, *9*, 5190−5196. (b) Dai, F. N.; He, H. Y.; Zhao, X. L.; Ke, Y. X.; Zhang, G. Q.; Sun, D. F. *CrystEngComm* **2010**, *12*, 337−340. (c) Zhang, L. L.; Liu, F. L.; Guo, Y.; Wang, X. P.; Guo, J.; Wei, Y. H.; Chen, Z.; Sun, D. F. *Cryst. Growth Des.* **2012**, *12*, 6215−6222.
(20) Spek, A. L. *Acta Crystallogr., Sect. A* **1990**, *46*, C34.
(21) Blatov, V. A. *Topos*; 2007; http://www.topos.ssu.samara.ru.
(22) (a) Wu, Q.; Esteghamatian, M.; Hu, N. X.; Popovic, Z.; Enright, G.; Tao, Y.; D'Iorio, M.; Wang, S. *Chem. Mater.* **2000**, *12*, 79−83. (b) McGarrah, J. E.; Kim, Y. J.; Hissler, M.; Eisenberg, R. *Inorg. Chem.* **2001**, *40*, 4510−4511. (c) Sun, D.; Zhang, N.; Huang, R. B.; Zheng, L. S. *Cryst. Growth Des.* **2010**, *10*, 3699−3709.
(23) (a) Wen, L.; Li, Y.; Lu, Z.; Lin, J.; Duan, C.; Meng, Q. *Cryst. Growth Des.* **2006**, *6*, 530. (b) Wen, L.; Lu, Z.; Lin, J.; Tian, Z.; Zhu, H.; Meng, Q. *Cryst. Growth Des.* **2007**, *7*, 93−99. (c) Niu, A.; Yang, J.; Guo, J.; Kan, W. Q.; Song, S. Y.; Du, P.; Ma, J. F. *Cryst. Growth Des.* **2012**, *12*, 2397−2410.
(24) Spek, A. L. *J. Appl. Crystallogr.* **2003**, *36*, 7−13.
(25) (a) Nijkamp, M. G.; Raaymakers, J. E. M. J.; Van Dillen, A. J.; De Jong, K. P. *Appl. Phys. A: Mater. Sci. Process.* **2001**, *72*, 619−623. (b) Han, D.; Jiang, F. L.; Wu, M. Y.; Chen, L.; Chen, Q. X.; Hong, M. C. *Chem. Commun.* **2011**, *47*, 9861−9863. (c) Rowsell, J. L. C.; Yaghi, O. M. *J. Am. Chem. Soc.* **2006**, *128*, 1304−1315. (d) Dailly, A.; Vajo, J. J.; Ahn, C. C. *J. Phys. Chem. B* **2006**, *110*, 1099−1101. (e) Suh, M. P.; Cheon, Y. E.; Lee, E. Y. *Chem.—Eur. J.* **2007**, *13*, 4208−4215.
(26) Czepirski, L.; Jagiello, J. *Chem. Eng. Sci.* **1989**, *44*, 797−801.
(27) (a) Phan, A.; Doonan, C. J.; Uribe-Romo, F. J.; Knobler, C. B.; O'Keefe, M.; Yaghi, O. M. *Acc. Chem. Res.* **2010**, *43*, 58−67. (b) Banerjee, R.; Furukawa, H.; Britt, D.; Knobler, C.; O'Keeffe, M.; Yaghi, O. M. *J. Am. Chem. Soc.* **2009**, *131*, 3875−3877. (c) Bloch, E. D.; Britt, D.; Lee, C.; Doonan, C. J.; Uribe−Romo, F. J.; Furukawa, H.; Long, J. R.; Yaghi, O. M. *J. Am. Chem. Soc.* **2010**, *132*, 14382−14384. (d) García-Ricard, O. J.; Hernández-Maldonado, A. J. *J. Phys. Chem. C* **2010**, *114*, 1827−1834. (e) Mulfort, K. L.; Farha, O. K.; Malliakas, C. D.; Kanatzidis, M. G.; Hupp, J. T. *Chem.—Eur. J.* **2010**, *16*, 276−281.

dx.doi.org/10.1021/ic501801f | *Inorg. Chem.* XXXX, XXX, XXX−XXX